Accelerated degradation testing and failure phenomenon of metalized film capacitors for AC filtering

Bo Yao
Department of Energy
Aalborg University
Aalborg, Denmark
ybo@energy.aau.dk

Yichi Zhang
Department of Energy
Aalborg University
Aalborg, Denmark
Yzhang@energy.aau.dk

Pedro Correia
Wind Systems A/S
Vestas
Aarhus, Denmark
paabc@vestas.com

Rui Wu
Wind Systems A/S
Vestas
Aarhus, Denmark
riwub@vestas.com

Sungyoung Song
Wind Systems A/S
Vestas
Aarhus, Denmark
suysn@vestas.com

Ionut Trintis
Wind Systems A/S
Vestas
Aarhus, Denmark
iotri@vestas.com

Haoran Wang
Intelligent Ind. Tech.
Three Gorges Co., Ltd
Wuhan, China
wang_haoran@ctg.com.cn

Huai Wang
Department of Energy
Aalborg University
Aalborg, Denmark
hwa@energy.aau.dk

2023 IEEE Applied Power Electronics Conference and Exposition (APEC) | 978-1-6654-7539-6/23/$31.00 ©2023 IEEE | DOI: 10.1109/APEC43580.2023.10131420

***Abstract*—This paper presents the degradation testing and failure mechanisms analysis of metalized film capacitors used for AC filtering in MW power converters. Based on more than 2,800 hours of accelerated testing under accelerated AC voltage, temperature, and AC current, various electro-thermal parameter data are recorded. The results reveal that capacitance values have negligible reduction until the testing samples catastrophically fail. The capacitor hot spot temperature and case temperature are measured along the testing, which are increasing. The observations provide a new perspective on the possible failure mechanisms and condition monitoring of film capacitors in AC filtering applications.**

***Keywords*—degradation testing, failure mechanism, metalized film capacitors, AC filtering, MW power converters, hot spot temperature**

I. Introduction

Metalized film capacitors are widely used in power electronic converters applications with high voltage and high ripple currents [1] [2]. The degradation of metalized film capacitors can lead to worse filtering capability and even severe catastrophe to the operating systems [3]-[5]. Accelerated testing is a significant method to investigate the aging mechanism and failure causes of film capacitors, and existing studies mostly focus on DC-link capacitors [6]-[10] and Electromagnetic Interference (EMI) suppression AC capacitors [11]-[13]. Although AC filtering film capacitors are indispensable components for AC industrial applications such as wind power and traction [14] [15], the existing literature still lacks studies and analyses on their degradation and failure.

In general, the degradation of metalized film DC capacitors can be characterized by a decrease in capacitance [6]-[10] and an increase in equivalent series resistance (ESR) [6] [9]. Some studies find that the degradation of metalized film EMI suppression AC capacitors can be manifested as a decrease in capacitance [11] [12] and an increase in ESR [11]. In [13], the decrease-slight in capacitance, and the increase-significant in loss factor are found for metalized film EMI suppression AC capacitors testing. However, these conventional studies cannot be easily extended to capacitors of other types and applications because the failure mechanism is affected by their specific design structure and stress conditions. Hence, for the aging mechanisms and failure characterization, the above conclusions from DC metalized film capacitors and EMI suppression AC capacitors need to be argued with caution for the validity of AC power filtering capacitors.

Based on the results of more than 2800 hours of accelerated aging testing in this paper: 1) The failure of AC filtering capacitors is mainly affected by temperature. When the temperature rise increases about 3 to 4 times than the initial temperature rise, the AC capacitor is failed. 2) The typical precursor, capacitance, hardly changes in the process of degradation when the applied AC voltage is within a certain range.

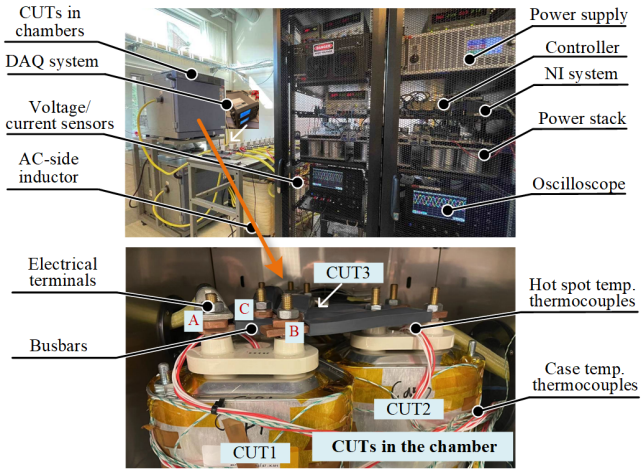

Fig. 1. Photo of the experiment platform.

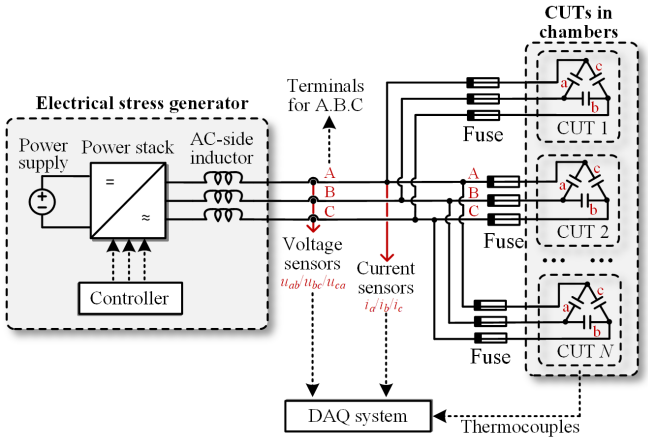

Fig. 2. Schematic diagram of the platform.

The structure of this paper is as follows: Section II presents the test configuration in the experiment; Section III gives the test results for capacitance and temperature, followed by the conclusions.

II. Test Configuration in the Experiment

The experimental platform and its schematic diagram are respectively shown in Fig. 1 and Fig. 2. The experimental platform consists of three main modules: the electrical stress generator, the capacitors under testing (CUTs) in the chamber, and the data acquisition system. The electrical stress generator is used to provide AC voltage and AC current for CUTs, which adopts a recently reported method that has the advantages of a minimum required power supply and is robust to testing sample degradation [16]. The CUTs are connected in the chamber by the busbars. The AC current and AC voltage of the CUTs are supplied by the electrical stress generator through the electrical terminals A.B.C.

It is worth noting that when a CUT is failed, a new

TABLE I. System and CUTs Parameters.

Stress emulation setup	
DC voltage of power supply U_{PS}	750 V
AC-side inductor L	2.5 mH
Switch frequency f_S	5000 Hz
CUTs setup for AC capacitors	
Capacitance of the CUT unit	75 μF
Rate AC ripple voltage (rms) U_R	750 V
Testing AC ripple voltage (rms) U_T	975 V (1.3×U_R)
Rate AC ripple current (rms) I_R	30 A
Testing AC ripple current (rms) I_T	39 A (1.3×I_R)
Testing ripple frequency f_R	50 Hz
Testing ambient temperture	87 °C

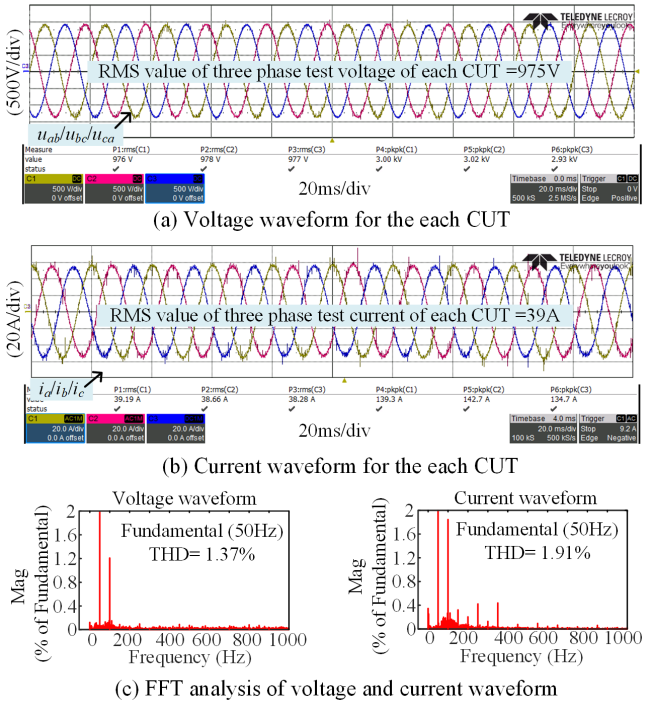

Fig. 3. Waveforms of voltage and current for CUTs.

CUT replaces it, while the other CUTs continue to be tested. Thermocouples are installed in the location of the hot spots and cases of the CUTs to obtain the hot spot temperature and case temperature. Therefore, the electrical stress and thermal stress data are collected in real-time by data acquisition (DAQ) systems [17] [18]. The a, b, and c represent three capacitor units for each CUT in Fig. 2. The main stress emulation and CUTs setup parameters are given in Table I. The ambient temperature is set to 87 °C, giving the CUTs an initial hot spot temperature of 100 °C. In this testing, the AC current (equivalent current from the terminals) and the AC voltage of each CUT are set with the 1.3 times acceleration factor. The fast Fourier transform (FFT) analysis in Fig. 3 shows that the AC voltage and current are mainly the fundamental

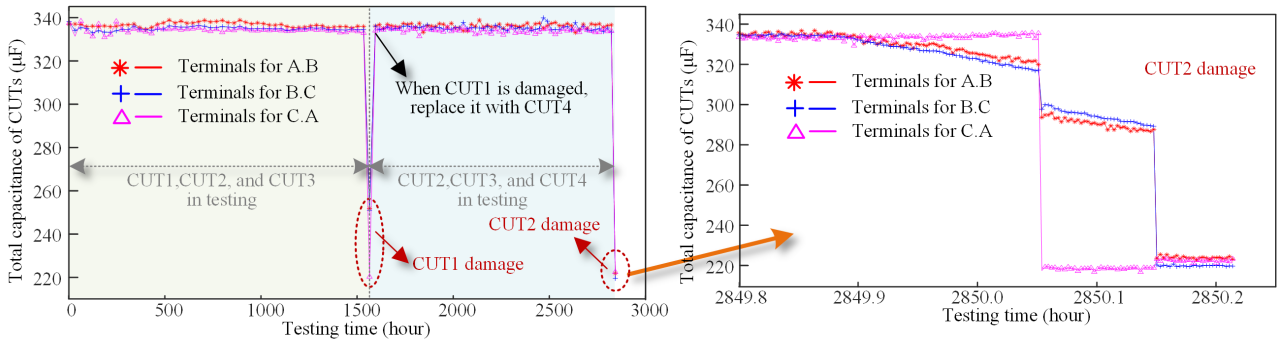

Fig. 4. Calculation results of capacitance for CUTs in testing time.

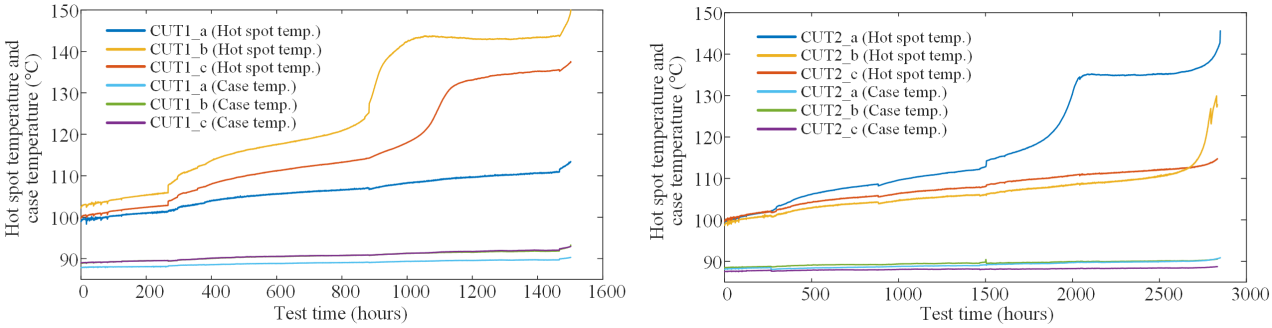

(a) Hot spot temperature and case temperature for CUT1

(b) Hot spot temperature and case temperature for CUT2

Fig. 5. Hot spot temperature and case temperature for CUT1 and CUT2.

components at 50 Hz with the THD value of less than 2%. The RMS value of AC voltage is maintained at 975 V, where the RMS value of AC current is 118 A.

III. Test Results

The accelerated degradation testing has lasted for more than 2800 h for CUTs, with CUT1 being failed after about 1550 h and CUT2 being failed after about 2850 h. In addition, CUT 3 still operates normally. This section shows test results and analysis of the electro-thermal stresses for CUTs.

A. Capacitance change and analysis

According to Fig. 3, ignoring the harmonic components of the AC voltage and current, the AC voltage U_{rms} and AC current I_{rms} (equivalent current from the terminals) of the CUTs at 50 Hz satisfy the following relationship:

$$\begin{aligned} U_{rms} &= I_{rms} \times Z_{cap} \\ &= I_{rms} \times \left(\frac{1}{2\pi f_R \times C} + R_s + 2\pi f_R \times L_s \right) \\ &\approx I_{rms} \times \frac{1}{2\pi f_R \times C} \end{aligned} \tag{1}$$

where Z_{cap}, L_s, R_s, and C represent the equivalent impedance, equivalent series inductance, equivalent series resistance, and capacitance of the CUTs, respectively. f_R is the ripple frequency for CUTs, which is 50 Hz in this paper.

Therefore, the capacitance of CUTs can be obtained in real-time:

$$C = \frac{I_{rms}}{2\pi f_{\mathrm{R}} \times U_{rms}} \tag{2}$$

The real-time capacitance results from three terminals of the overall CUTs can be obtained according to the calculation of (2), as shown in Fig. 4. The capacitance of CUTs hardly changes during the test time before they are failed. According to the calculation results of the capacitance of CUT2 for 0.5 hours before and after the failure, the capacitance of the CUT2 drops rapidly from the normal capacitance to zero in a short period of time (about 10 minutes) before the failure. This happens because the CUTs are equipped with an overpressure mechanism that disconnects the terminals and not because of the winding total failure.

B. Temperature change and analysis

The hot spot temperature, case temperature, and temperature rise from hot spot to case of three capacitor units a, b, and c in CUT1 and CUT2 are given in Fig. 5, where the ambient temperature is kept at a constant level by the climate chamber. From the results, the hot spot temperature and temperature rise

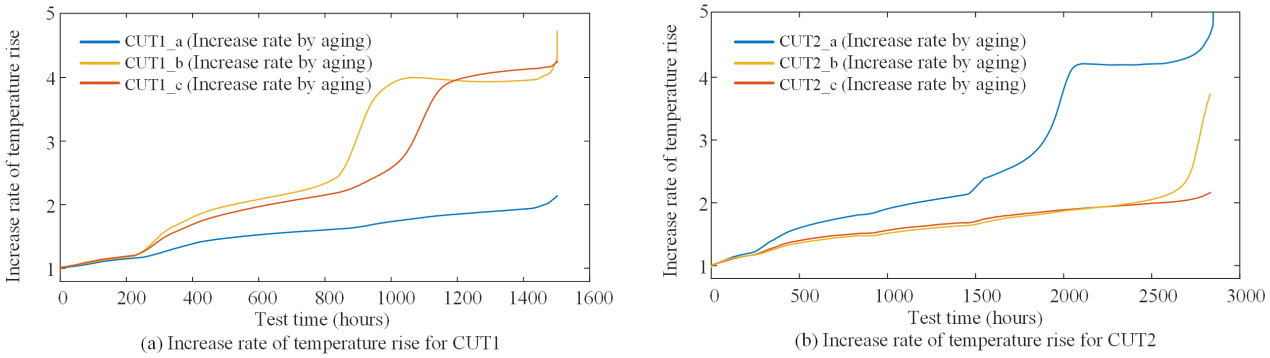

(a) Increase rate of temperature rise for CUT1

(b) Increase rate of temperature rise for CUT2

Fig. 6. Increase rate of temperature rise from hot spot to case for CUT1 and CUT2.

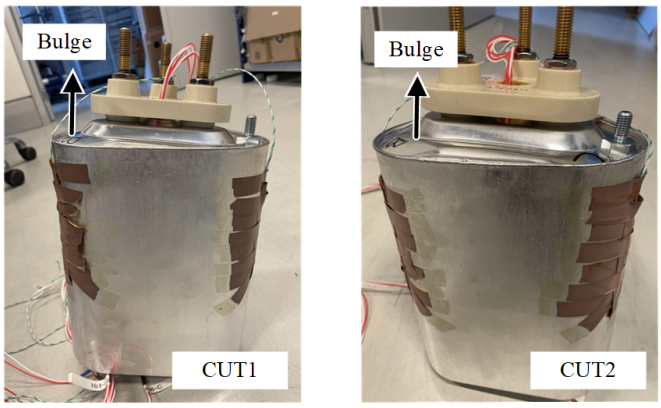

(a) CUT1 surface

(b) CUT2 surface

Fig. 7. Surface pictures of failed CUTs.

of each capacitor unit gradually increase with the test time. When the hot spot temperature of one capacitor unit of the CUTs reaches about 140 °C, the capacitor is failed.

The temperature rises T_{rise} and its increase rate RT_{rise} of CUTs from the case to the hot spot can be respectively expressed as [19] [20]:

$$\begin{cases} T_{rise} = T_{\text{hot}} - T_{\text{case}} = P_{\text{loss}} R_{\text{th}} \\ RT_{rise} = \frac{T_{\text{rise}}(t)}{T_{rise(0)}} \end{cases} \tag{3}$$

where T_{hot} , T_{case} , P_{loss} , R_{th} , and $T_{rise(0)}$ represent the hot spot temperature, case temperature, power loss of thermal resistance, and initial temperature rise of the CUTs, respectively.

The increased rate of temperature rise for CUTs is given in Fig. 6. The aging of the AC power filtering capacitor can be characterized by the temperature rise from hot spot to case. The results show that the value of the temperature rise increases to about 3 to 4 times when the AC capacitor is failed.

C. Physical characterization of failure

Fig. 7 illustrates the surface behavior of the CUTs after failure. It can be seen that when the AC filter capacitors fail catastrophically, the top of the capacitors expand and bulge.

These behaviors indicate that during the degradation of the AC capacitor, the dielectric film does not break down, and thus the capacitance has negligible reduction until the testing samples catastrophically fail. Since there is no DC voltage component in the AC capacitor, the rated AC voltage of 1.3 times the acceleration factor applied in this paper does not reach the critical value of dielectric film breakdown, so the test results in Fig. 4 show that the capacitance has negligible reduction before they are catastrophically failed. The possibility of capacitor catastrophic failure greatly increases when the hot spot temperature exceeds the melting point temperature of the dielectric film (about 140°C for polypropylene). The burning film makes the top of the capacitors expand and bulge.

IV. Conclusions

This paper investigates the failure mechanisms of a type of AC power filtering film capacitors used for MW power converters. Based on the results of more than 2800 hours of accelerated aging testing, the following conclusions are obtained: 1) The failure of AC power filtering capacitors is mainly affected by the increasing of hot spot temperature. When the hot spot temperature rises to about 140 °C and the temperature rise rate increases to about 4 to 5 times, the possibility of AC capacitor failure greatly increases. 2) The capacitance values have negligible reduction until the testing samples catastrophically fail when the applied AC voltage is within a certain range (the acceleration factor of the applied AC voltage is 1.3 in this paper), which means that the capacitance is not suitable for a common precursor abled to characterize degradation.

References

[1] H. Wang and F. Blaabjerg, “Reliability of capacitors for DC-link applications in power electronic converters—an overview,” *IEEE Trans. Ind. Appl.*, vol. 50, no. 5, pp. 3569–3578, Sep./Oct. 2014.

[2] M. Bramoulle, "Electrolytic or film capacitors?" in *Proc. IEEE Ind. Appl. Conf., St. Louis, MO, USA*, vol. 2, 1998, pp. 1138–1141 vol.2.

[3] S. Liu, Z. Shen, and H. Wang, "Safe operating area of DC-link film capacitors," *IEEE Trans. Power Electron.*, vol. 36, no. 10, pp. 11 014–11 018, Oct. 2021.

[4] H. Wang, M. Liserre, and F. Blaabjerg, "Toward reliable power electronics: Challenges, design tools, and opportunities," *IEEE Ind. Electron. Mag.*, vol. 7, no. 2, pp. 17–26, Jun. 2013.

[5] H. Li, Y. Chen, F. Lin, B. Peng, F. Lv, M. Zhang, and Z. Li, "The capacitance loss mechanism of metallized film capacitor under pulsed discharge condition," *IEEE Trans. Dielectr. Electr. Insul.*, vol. 18, no. 6, pp. 2089–2094, Dec. 2011.

[6] M. Makdessi, A. Sari, and P. Venet, "Metallized polymer film capacitors ageing law based on capacitance degradation," *Microelectron. Rel.*, vol. 54, no. 9-10, pp. 1823–1827, Jul. 2014.

[7] M. Makdessi, A. Sari, P. Venet, P. Bevilacqua, and C. Joubert, "Accelerated ageing of metallized film capacitors under high ripple currents combined with a DC voltage," *IEEE Trans. Power Electron.*, vol. 30, no. 5, pp. 2435–2444, May 2015.

[8] W. Zhou, M. Wang, Q. Wu, L. Xi, K. Xiao, K. P. Bhat, and C. Chen, "Accelerated life testing method of metallized film capacitors for inverter applications," *IEEE Trans. Transport. Electrific.*, vol. 7, no. 1, pp. 37–49, Mar. 2021.

[9] H. Wang, D. A. Nielsen, and F. Blaabjerg, "Degradation testing and failure analysis of DC film capacitors under high humidity conditions," *Microelectron. Rel.*, vol. 55, no. 9-10, pp. 2007–2011, Aug./Sep. 2015.

[10] R. Gallay, "Metallized film capacitor lifetime evaluation and failure mode analysis," *arXiv preprint arXiv:1607.01540*, 2016.

[11] J. Kirchhof and S. Kitterer, "Degradation from metallized polymer film capacitors with the dielectric polypropylene under the influence of humid heat," in *Proc. Int. Exhib. Conf. Power Electron., Intell. Motion, Renew. Energy Energy Manag.*, 2015, pp. 1–8.

[12] H. Li, P. Lewin, and J. C. Fothergill, "Aging mechanisms of X2 metallized film capacitors in a high temperature and humidity environment," in *n Proc. IEEE Int. Conf. Dielectr. (ICD)*, vol. 2, 2016, pp. 804–807.

[13] P. Mach and M. Horák, "Analysis of changes due to long-term thermal aging in capacitors manufactured from polypropylene film," in *Proc. 43rd Int. Spring Seminar Electron. Technol. (ISSE)*, 2020, pp. 1–5.

[14] "Heavy Duty Three-phase AC Filter Capacitors." Electronicon, https://www.powercapacitors.info/download/200.003-020051_E62-3ph.pdf, 2018.

[15] D. Zhou, Y. Song, Y. Liu, and F. Blaabjerg, "Mission profile based reliability evaluation of capacitor banks in wind power converters," *IEEE Trans. Power Electron.*, vol. 34, no. 5, pp. 4665–4677, May 2019.

[16] B. Yao, Q. Wang, H. Wang, K. Hasegawa, and H. Wang, "A robust testing method for DC and AC capacitors with minimum required power supply," *IEEE Trans. Power Electron.*, vol. 37, no. 5, pp. 4942–4946, May 2022.

[17] "CompactRIO Systems." NATIONAL INSTRUMENTS, https://www.ni.com/da-dk/shop/compactrio.html, 2022.

[18] "DAQ970A Data Acquisition System." Keysight Technologies, https://www.keysight.com/us/en/assets/7018-06259/technical-overviews/5992-3168.pdf, 2021.

[19] B. Yao, X. Ge, D. Xie, S. Li, Y. Zhang, H. Wang, and H. Wang, "Electrothermal stress analysis and lifetime evaluation of dc-link capacitor banks in the railway traction drive system," *IEEE J. of Emerg. Se. Topics in Power Electron.*, vol. 9, no. 4, pp. 4269–4284, 2021.

[20] C. Lv, J. Liu, Y. Zhang, J. Yin, R. Cao, Y. Li, and X. Liu, "A method to characterize the shrinking of safe operation area of metallized film capacitor considering electrothermal coupling and aging in power electronics applications," *IEEE Trans. Ind. Electron.*, 2022 (Early Access).